Electronic Supplementary Material (ESI) for Journal of Materials Chemistry A.

Highly Efficient Catalysis for Oxygen Reduction using Well-dispersed Iron Carbide Nanoparticles Embedded in the Multichannel Hollow Nanofibers

Hongyin Xia[ab], Shan Zhang[a], Xiaoqing Zhu[a], Huanhuan Xing[a], Yuan Xue[ab], Bolong Huang[c*], Mingzi Sun[c], Jing Li[a*], and Erkang Wang[a*]

[a] State Key Laboratory of Electroanalytical Chemistry, Changchun Institute of Applied Chemistry, Chinese Academy of Sciences, 5625 Renmin Street, Changchun, Jilin 130022, China.

[b] University of Science and Technology of China, Hefei, Anhui, 230026, China.

[c] Department of Applied Biology and Chemical Technology, The Hong Kong Polytechnic University, Hung Hom, Kowloon, Hong Kong SAR, China.

Equations in Electrochemical characterization

The H_2O_2 yield and the number of electron transfer (n) were calculated with the following equations:

$$H_2O_2\% = \frac{200 \times I_r/N}{I_d + I_r/N} \quad (1)$$

$$n = \frac{4I_d}{I_d + I_r/N} \quad (2)$$

where I_d is the disk current, I_r is the ring current, and N (0.37) is the collection efficiency of the rotating ring-disk electrode (RRDE).

Koutecky-Levich equations:

$$\frac{1}{J} = \frac{1}{J_l} + \frac{1}{J_k} = \frac{1}{B\omega^{0.5}} + \frac{1}{J_k} \quad (3)$$

$$B = 0.62nFC_0(D_0)^{2/3}V^{-1/6}$$

where J is the recorded current density, J_K is the kinetic-limiting current density, J_L is the diffusion-limiting current density, ω is the electrode rotating speed in rad s^{-1}, F is the Faraday constant (96485 C mol^{-1}), C_0 is the bulk concentration of O_2 in 0.10 M KOH solution (1.2×10^{-6} mol cm^{-3}), D_0 is the diffusion coefficient of O_2 (1.9×10^{-5} cm^2 s^{-1}), and V is the kinematic viscosity of 0.10 M KOH solution (0.01 cm^2 s^{-1}). The K-L plots ($\omega^{-1/2}$ vs J^{-1}) in O_2-saturated 0.1 M KOH can be derived from LSV curves at various rotation speeds and different potentials.

Calibrate to reversible hydrogen electrode (RHE)

In all measurements, we used Hg/HgO electrode as the reference electrode. It was calibrated with respect to RHE. The calibration was performed in the high purity H_2 saturated electrolyte with a Pt wire as the working electrode. CVs were run at a scan rate of 1 $mV \cdot s^{-1}$, and the average of the two potentials at which the current crossed zero was taken to be the thermodynamic potential for the hydrogen electrode reactions. In 0.1 M KOH, E (RHE) = E (Hg/HgO) + 0.879 V. All the potentials reported in this manuscript were against RHE.

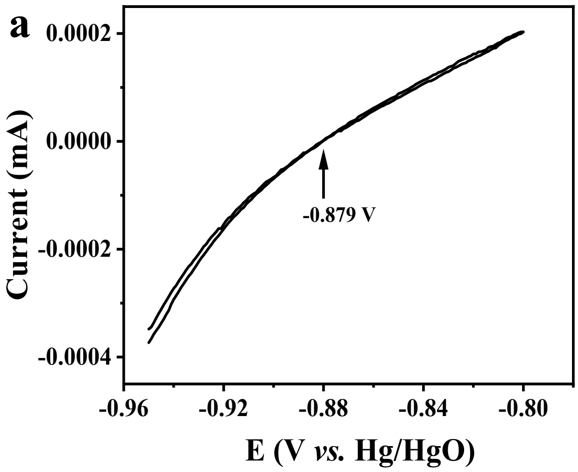

Figure S1. (a) Calibration of the reference electrode against the RHE.

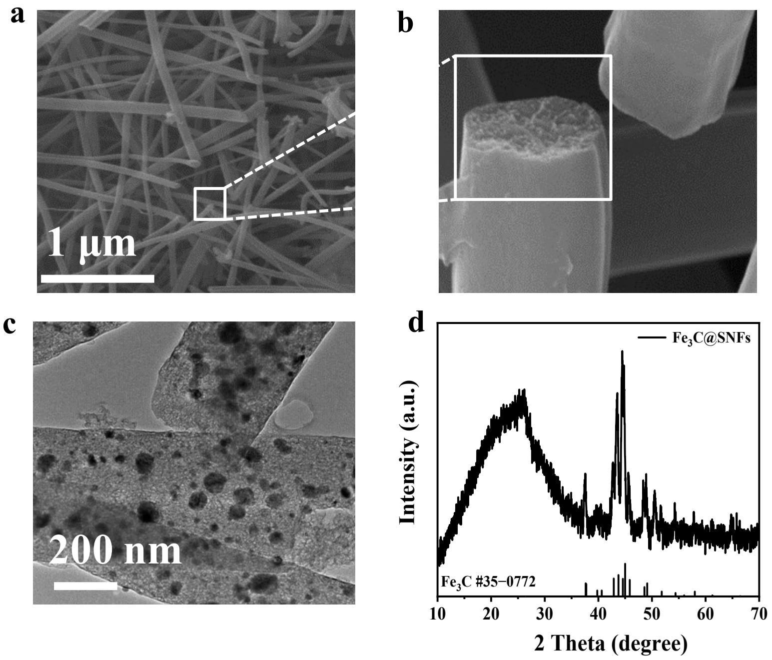

Figure S2. (a and b) SEM, (c) TEM images (d) XRD of Fe_3C@SNFs.

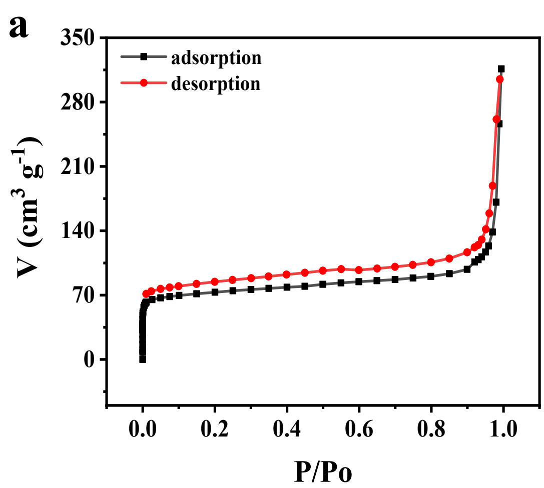

Figure S3. (a) Nitrogen adsorption-desorption isotherms for the Fe_3C@SNFs.

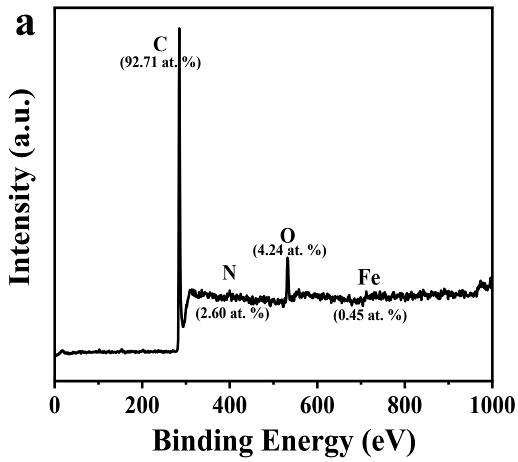

Figure S4. (a) XPS survey for the Fe_3C@MHNFs.

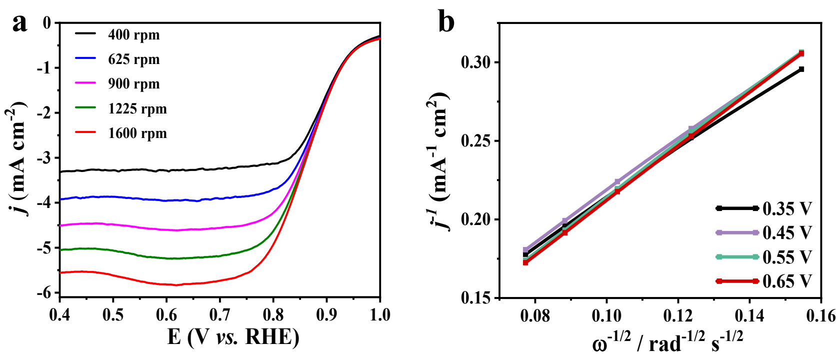

Figure S5. (a) LSV curves of Fe_3C@MHNFs at different rotating speeds, (b) the corresponding K-L plots.

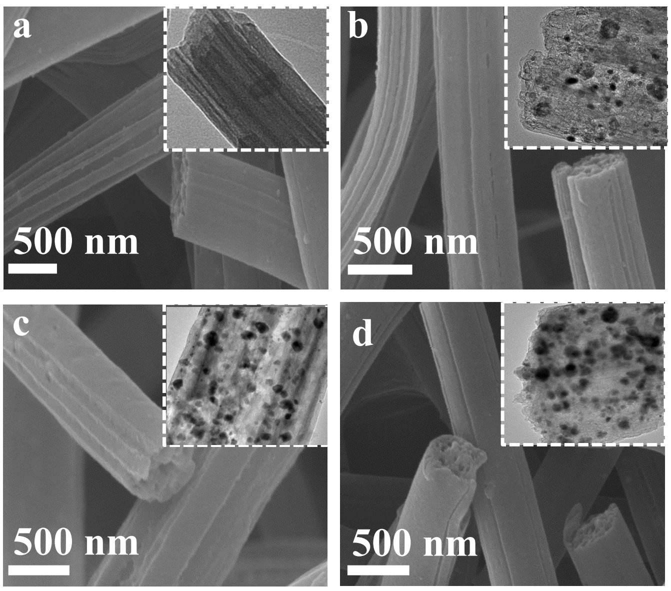

Figure S6. SEM and TEM for (a) MHNFs, (b) Fe_3C-1@MHNFs, (c) Fe_3C@MHNFs, (d) Fe_3C-3@MHNFs.

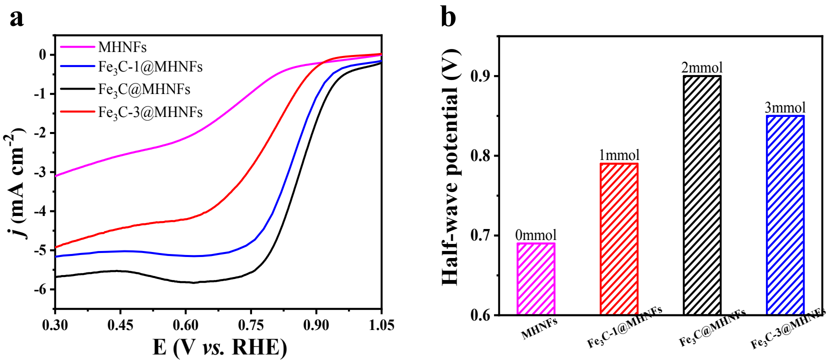

Figure S7. (a) Polarization curves and (b) $E_{1/2}$ of the MHNFs, Fe_3C-1@MHNFs, Fe_3C@MHNFs and Fe_3C-3@MHNFs.

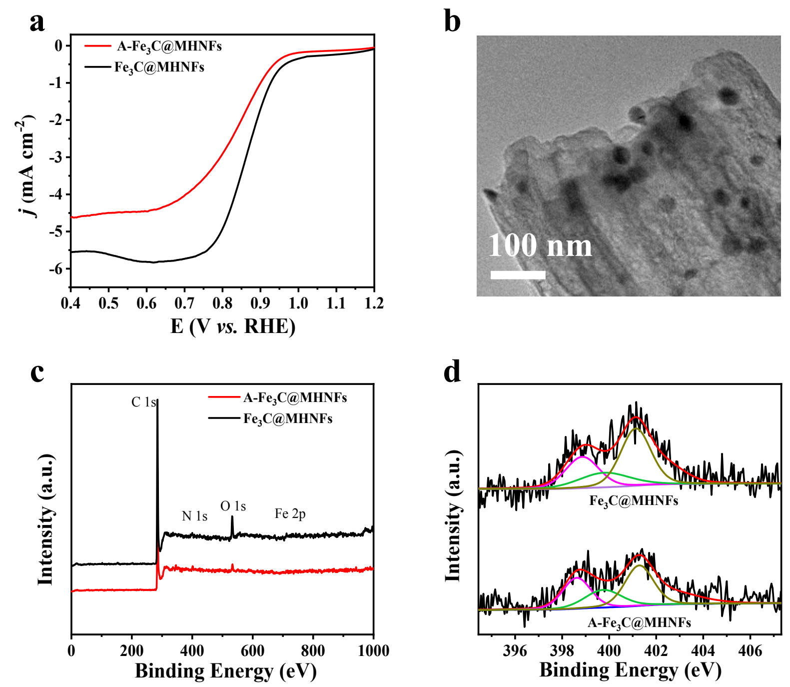

Figure S8. (a) Polarization curves of Fe_3C@MHNFs and A-Fe_3C@MHNFs; (b) TEM image of A-Fe_3C@MHNFs; (c) XPS survey, (d) N 1s XPS spectra of Fe_3C@MHNFs and A-Fe_3C@MHNFs.

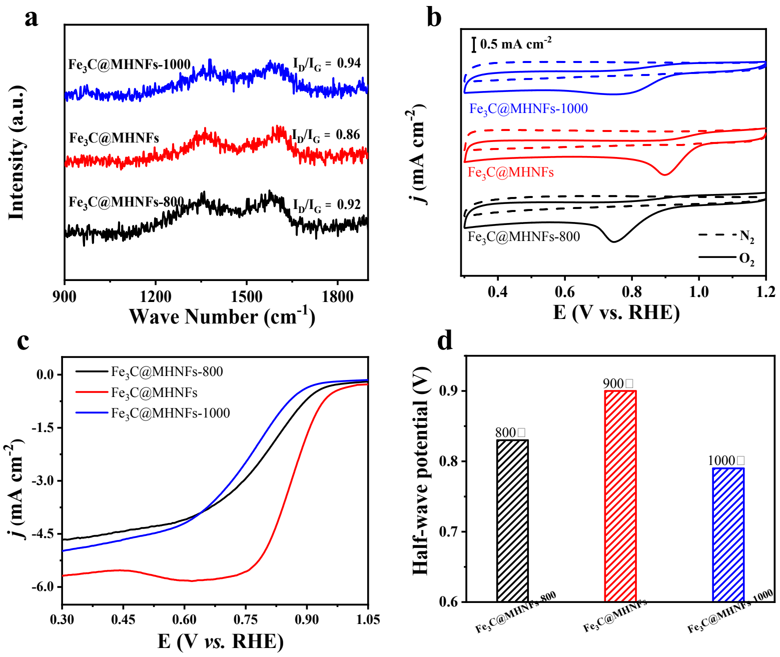

Figure S9. (a) Raman; (b) CV curves; (c) Polarization curves; (d) $E_{1/2}$ of Fe_3C@MHNFs-800, Fe_3C@MHNFs and Fe_3C@MHNFs-1000.

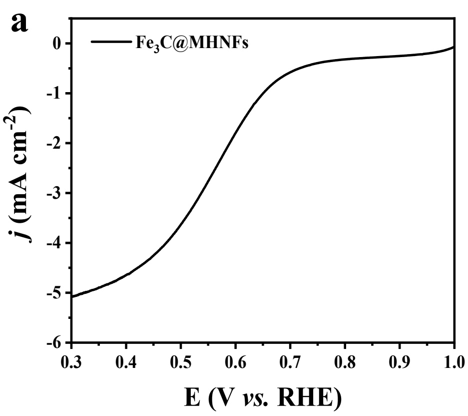

Figure S10. (a) LSV curves of Fe_3C@MHNFs in 0.5 M H_2SO_4.

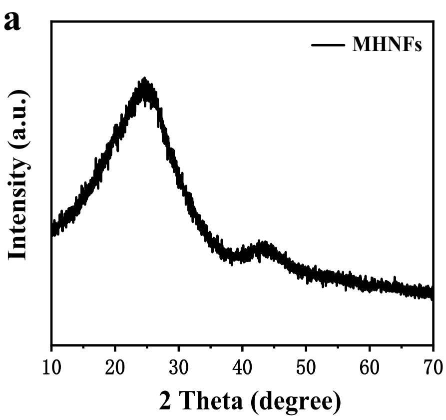

Figure S11. (a) XRD of the MHNFs.

Table S1. Comparison of the ORR activities of Fe_3C@MHNFs with the noble-metal-free catalysts literature-reported.

Catalyst	Electrolyte	$E_{1/2}$ (V vs. RHE)	Catalyst loading (mg cm^{-2})	References
Fe_3C@MHNFs	0.1 M KOH	0.90	0.20	This work
Fe-N/C-800	0.1 M KOH	0.80	0.10	1
BCNFNHs	0.1 M KOH	0.86	1.20	2
Fe@C-FeNC	0.1 M KOH	0.89	0.70	3
C-FeZIF-900-0.84	0.1 M KOH	0.84	0.50	4
HP-Fe-N/CNFs	0.1 M KOH	0.81	0.25	5
Fe-NMP	0.1 M KOH	0.65	0.25	6
Fe/N/S-CNTs	0.1 M KOH	0.88	0.50	7
Fe14NDC-9	0.1 M KOH	0.88	0.25	8

Table S2. XPS of Fe_3C@MHNFs synthesized with ammoniation and A-Fe_3C@MHNFs synthesized without ammoniation.

Samples	C (at%)	N (at%)	O (at%)	Fe (at%)	pyridinic N (%)	pyrrolic N (%)	graphitic N (%)
Fe_3C@MHNFs	92.71	2.60	4.24	0.45	0.30	0.21	0.49
A-Fe_3C@MHNFs	93.08	1.21	5.30	0.41	0.23	0.29	0.48

Reference

1. L. Lin, Z. Qing and A.-W. Xu, *J. Am. Chem. Soc.*, 2015, **249**, 11027-11033.
2. W. Yang, X. Liu, X. Yue, J. Jia and S. Guo, *J. Am. Chem. Soc.*, 2015, **137**, 1436-1439.
3. W.-J. Jiang, L. Gu, L. Li, Y. Zhang, X. Zhang, L.-J. Zhang, J.-Q. Wang, J.-S. Hu, Z. Wei and L.-J. Wan, *J. Am. Chem. Soc.*, 2016, **138**, 3570-3578.
4. Y. Deng, Y. Dong, G. Wang, K. Sun, X. Shi, L. Zheng, X. Li and S. Liao, *ACS Appl. Mater. Interfaces*, 2017, **9**, 9699-9709.
5. Y. Zhao, Q. Lai, Y. Wang, J. Zhu and Y. Liang, *ACS Appl. Mater. Interfaces*, 2017, **9**, 16178-16186.
6. M. M. Hbssen, K. Artyushkova, P. Atanassov and A. Serov, *J. Power Sources*, 2018, **375**, 214-221.
7. H. Jin, H. Zhou, W. Li, Z. Wang, J. Yang, Y. Xiong, D. He, L. Chen and S. Mu, *J. Mater. Chem. A*, 2018, **6**, 20093-20099.
8. M. Hoque, S. Zhang, M. L. Thomas, Z. Li, S. Suzuki, A. Ando, M. Yanagi, Y. Kobayashi, K. Dokko and M. Watanabe, *J. Mater. Chem. A*, 2018, **6**, 1138-1149.